

Dust charging processes with a Cairns-Tsallis distribution function with negative ions

A. A. Abid,^{1,a)} M. Z. Khan,^{1,2,b)} S. L. Yap,² H. Terças,^{3,c)} and S. Mahmood⁴

¹Applied Physics Department, Federal Urdu University of Arts, Science and Technology, Islamabad Campus, Islamabad 45320, Pakistan

²Plasma Technology Research Center, Department of Physics, Faculty of Science, University of Malaya, Kuala Lumpur 50603, Malaysia

³Physics of Information Group, Instituto de Telecomunicações, Av. Rovisco Pais, Lisbon 1049-001, Portugal

⁴Science Place, University of Saskatchewan, Saskatoon, Saskatchewan S7N5A2, Canada

(Received 10 October 2015; accepted 5 January 2016; published online 22 January 2016)

Dust grain charging processes are presented in a non-Maxwellian dusty plasma following the Cairns-Tsallis (q, α)–distribution, whose constituents are the electrons, as well as the positive/negative ions and negatively charged dust grains. For this purpose, we have solved the current balance equation for a negatively charged dust grain to achieve an equilibrium state value (viz., $q_d = \text{constant}$) in the presence of Cairns-Tsallis (q, α)–distribution. In fact, the current balance equation becomes modified due to the Boltzmannian/streaming distributed negative ions. It is numerically found that the relevant plasma parameters, such as the spectral indexes q and α , the positive ion-to-electron temperature ratio, and the negative ion streaming speed (U_0) significantly affect the dust grain surface potential. It is also shown that in the limit $q \rightarrow 1$ the Cairns-Tsallis reduces to the Cairns distribution; for $\alpha = 0$ the Cairns-Tsallis distribution reduces to pure Tsallis distribution and the latter reduces to Maxwellian distribution for $q \rightarrow 1$ and $\alpha = 0$. © 2016 AIP Publishing LLC.

<http://dx.doi.org/10.1063/1.4940329>

I. INTRODUCTION

Recently, there has been a great deal of interest in understanding different types of collective processes in dusty plasmas (an admixture of such massive and either negatively or positively charged dust, electrons, ions, and neutral species), because of their important role in astrophysical and space environments,¹ such as asteroid zones, planetary atmospheres, interstellar media, accretion disks, dark molecular clouds, cometary tails, nebulae, the Earth's environment,^{2,3} and also in industrial plasmas.⁴ On the other hand, it has been shown—both theoretically and experimentally—that the dust charge dynamics introduces new eigenmodes.^{5–8} The celebrated dust acoustic mode,^{7,9–11} where the dust particle mass provides the inertia and the pressure of electrons and ions give rise to the restoring force, is a good example. Rao *et al.*⁵ theoretically predicted the existence of an extremely low-phase-velocity (in comparison with both the electron and ion thermal velocities) dust acoustic waves in an unmagnetized dusty plasma. The laboratory experiments of Barkan *et al.*⁷ and D'Angelo¹¹ have conclusively verified this theoretical prediction and have shown some nonlinear features of dust acoustic waves.

In typical experimental conditions, dust grains are immersed in an ambient plasma and radiative background. Their interaction with the other plasma particles (namely, electrons and ions) is due to the charge that they carry. Dust

grains are charged by a number of competing processes, depending upon local conditions, such as photoelectric emission stimulated by ultraviolet radiation, collisional charging by electrons and ions, and disruption and secondary emission due to Maxwellian stress.^{12–16} In fact, massive dust particles can collect a large amount of the highly mobile plasma electrons and the dust grain generally attains negative charge. The fluctuating microscopic electron and ion currents flowing onto the surface of the individual grains result in dust-charge variation. In the steady state, the electron and ion grain currents are equal and determine the equilibrium dust charge. In 1994, the dust charging phenomena were hypothesized to be due to the bombardment of electrons and positive ions¹⁷ to examine dust grain surface potential, both theoretically and experimentally. Later on, these works were extended^{18,19} to highlight the role of negative ions in the Maxwellian and non Maxwellian κ –distributed plasmas.

A new distribution designed to model superthermal particles observed by the Viking spacecraft²⁰ and Freja satellite²¹ was introduced by Cairns *et al.*²² It was represented in terms of a parameter α , which calculates deviation from the Maxwellian distribution function. As a consequence, it was shown that the nature of ion-sound solitary structures can change in the presence of nonthermal electrons, producing nonlinear solitary waves that may have either an enhanced or depleted density. A subsequent series of studies have later employed the Cairns model.^{23–26} For example, Verheest and Pillay²⁷ investigated large amplitude dust-acoustic solitary waves in plasmas with negatively charged cold dust and either nonthermally distributed ions or electrons. Later on,

^{a)}Electronic mail: abidaliabid1@hotmail.com

^{b)}Electronic mail: mzk_qau@yahoo.com

^{c)}Electronic mail: hugo.tercas@tecnico.ul.pt

Verheest and Hellberg²⁸ investigated large ion acoustic solitary waves and double layers in plasmas with positive ions and nonthermal electrons. Both studies detailed the conditions under which such structures are to be generated. Moreover, Mamun and co-workers have investigated the combined effect of positively charged dust particles and the nonthermal electrons in dust-ion-acoustic solitary waves,^{29,30} and the nonthermal ions in dust-acoustic waves.³¹

Over the last few years, the non-extensive statistical mechanics based on the deviations of Boltzmann-Gibbs-Shannon (BGS) entropic measure has been paid a great deal of attention. In statistical mechanics, extensive thermodynamical quantities are proportional to amount of matter present or system size such as volume V , particle number N , total internal energy E , magnetization M , etc. Thus, if we double the number of particles in a certain thermodynamic system, the total energy, for example, will also double as a consequence of extensivity. Non-extensive quantities, however, such as pressure P , temperature T , and chemical potential μ , are independent of the total amount of matter. Moreover, the ratio of two extensive quantities results in a non-extensive quantity, such as the number density $n = N/V$, which is the ratio of the number of particle to volume of the system.

A suitable non-extensive generalization of the BGS entropy for statistical equilibrium was first proposed by Renyi and later investigated by Tsallis,³² extending the standard additivity of the entropies to the nonlinear, non-extensive case where one particular parameter, the entropic index q , characterizes the degree of non-extensivity of system considered (in this representation, the Maxwell-Boltzmann distribution is recovered in the limit $q \rightarrow 1$). Two important physical regions can be identified: the region $-1 < q \leq 1$, covering all velocities (and potentially representing the high-energy tails); and the region $q \geq 1$, where the distribution function exhibits a thermal cut-off on the maximum value allowed for the velocity of the particles.³³ The ion acoustic dynamics in plasmas³⁴⁻³⁶ has also been investigated in the context of the Tsallis model. Tribeche *et al.*³⁷ considered ion-acoustic solitary wave generation in a

two-component plasma with Tsallis-distributed electrons, where it showed the emergence of both compressive and rarefactive solitons. Alternatively, a κ -distribution can be used to model the plasma behavior, as described by Vasyliunas.³⁸ Interestingly, it has been argued that the κ -distribution can be derived from the Tsallis distribution.³⁹ The most latest non-Maxwellian distribution termed as Vasyliunas-Cairns distribution was investigated by Abid *et al.*⁴⁰

This manuscript is organized as follows: In Sec. II, we critically examine the Cairns-Tsallis (q, α)-distribution function and place limits on its range of validity in general and specifically for application to soliton studies. In Sec. III, we obtain the charging currents on the dust grain surface due to Cairns-Tsallis-distributed plasma species, i.e., electrons and positive/negative ions. In the steady state, the dust charging equation reduces to the current balance equation, which can be employed to study the dust grain surface potential and the dust grain charging mechanism in the presence of streaming of negative ions. Finally, numerical results are discussed and summarized in Sec. IV.

II. THE CAIRNS-TSALLIS DISTRIBUTION AND ITS RANGE OF VALIDITY

Three dimensional hybrid Cairns-Tsallis (q, α)-distribution, which is specifically a product of the Cairns and the Tsallis distribution functions, is given⁴¹ by

$$f_{CT}(\mathbf{V}_j) = C_{q\alpha} \left(1 + \alpha \frac{V_j^4}{V_{Tj}^4} \right) \left[1 - (q-1) \frac{V_j^2}{2V_{Tj}} \right]^{\frac{1}{q-1}}, \quad (1)$$

where $V_{Tj} = (T_j/m_j)^{1/2}$ is thermal velocity of j th species ($j = e$ for electron, i for ions, and n for negative ions), and q and α are real parameters, associated with the so-called nonextensivity and the number of nonthermal electrons, positive ions, and negative ions in the distribution, respectively. Furthermore, $C_{q\alpha}$ is a constant of normalization given by⁴²

$$C_{q\alpha} = \frac{1}{(2\pi V_{Tj})^{\frac{3}{2}}} \left[\frac{\Gamma\left(\frac{1}{1-q}\right) (1-q)^{\frac{5}{2}}}{\Gamma\left(\frac{1}{1-q} - \frac{5}{2}\right) \left[3\alpha + \left(\frac{1}{1-q} - \frac{3}{2}\right) \left(\frac{1}{1-q} - \frac{5}{2}\right) (1-q)^2 \right]} \right] \quad \text{for } -1 < q \leq 1,$$

$$C_{q\alpha} = \frac{1}{(2\pi V_{Tj})^{\frac{3}{2}}} \left[\frac{\Gamma\left(\frac{1}{1-q} + \frac{5}{2}\right) (q-1)^{\frac{5}{2}} \left(\frac{1}{q-1} + \frac{3}{2}\right) \left(\frac{1}{q-1} + \frac{5}{2}\right)}{\Gamma\left(\frac{1}{q+1} + 1\right) \left[3\alpha + \left(\frac{1}{q-1} + \frac{3}{2}\right) \left(\frac{1}{q-1} + \frac{5}{2}\right) (q-1)^2 \right]} \right] \quad \text{for } q \geq 1.$$

Here, m_j is the mass and T_j the temperature of j th species ($j = e, i, n$) and $\Gamma(x)$ is the Gamma function. In the limit $q \rightarrow 1$, both expressions convert into the Cairns distribution.²² For $\alpha = 0$, Eq. (1) reduces to pure Tsallis distribution.³² In the

particular case $\alpha = 0$ and $q \rightarrow 1$, the Cairns-Tsallis distribution exactly reduces to the Maxwellian distribution. It is observed that the pure Tsallis distribution function behaves very differently in the two ranges, $-1 < q < 1$ and $q > 1$.³³ In

the former range, the distribution is nonzero over the full range of velocities from $-\infty$ to $+\infty$, and it reflects an excess of superthermal particles in the non-Maxwellian tail. It is, thus, in principle, similar to a power-law or a κ -distribution in that sense. On the other hand, for $q > 1$, it exhibits a thermal cutoff, is zero in the region $|V_{Tj}| > (T_j/m_j)^{1/2}$, and it is, thus, bounded by the thermal velocity. Hence, it follows that the product Cairns-Tsallis distribution is zero beyond the thermal speed, and in that q range is not of any interest for the representation of the commonly observed non-Maxwellian tail distributions.

III. DUST POTENTIAL VARIATION WITH CAIRNS-TSALLIS DISTRIBUTION FUNCTION

We consider that finite-sized dust grains are immersed in an unmagnetized plasma, containing electrons and positive/negative ions following the Cairns-Tsallis-distribution. We further assume that the plasma particles approach the dust grain from an infinite distance. When they enter the Debye sphere, due to the electrostatic force between the dust grain and the plasma species, a negative charge on dust surface is accumulated. Here, $\partial q_d/\partial t = \sum_j I_j^{q\alpha}$ is the basic charging equation for dust grain due to the electrons and positive/negative ions. In steady state value ($q_d = \text{const.}$), the current balance equation can be expressed as⁴³

$$I_e^{q\alpha} + I_i^{q\alpha} + I_n^{q\alpha} = 0, \quad (2)$$

with

$$Q = \left[\frac{\Gamma\left(\frac{1}{1-q}\right)(1-q)^{\frac{5}{2}}}{\Gamma\left(\frac{1}{1-q} - \frac{5}{2}\right) \left[3\alpha + \left(\frac{1}{1-q} - \frac{3}{2}\right) \left(\frac{1}{1-q} - \frac{5}{2}\right) (1-q)^2 \right]} \right], \quad \text{for } -1 < q \leq 1.$$

Here, Z_i (Z_n) is the positive (negative) ion charging state, and n_j is plasma number density of j -th species. For $\alpha = 0$, and $q \rightarrow 1$, the values of $A_{q\alpha}$, $B_{q\alpha}$, and Q approach to 1 and the electron current, the positive ion current, and the negative ion current reduce to Maxwellian current.¹⁸ Now, using the relation $\phi_d = q_j/r_d$, and the charge-neutrality condition $n_e - Z_i n_i + Z_n n_n = q_d n_d e$, we insert Eqs. (4)–(6) into Eq. (2) to determine the equilibrium dust grain surface potential as

$$\begin{aligned} & \sqrt{\sigma} - \frac{A_{q\alpha} Z_i U}{B_{q\alpha} \sqrt{\sigma}} - \mu \left(1 - \rho \frac{Z_n}{Z_i} + Z_i P U \right) \exp\left(\frac{A_{q\alpha} U}{B_{q\alpha}}\right) \\ & = \rho \beta \sqrt{\gamma} \frac{Z_n}{Z_i} \left(1 + \frac{A_{q\alpha} Z_n U}{B_{q\alpha} \gamma} \right). \end{aligned} \quad (7)$$

Here, $\sigma = T_i/T_e$, $\mu = (m_i/m_e)^{1/2}$, $\rho = n_n/n_i$, $\beta = (m_i/m_n)^{1/2}$, and $\gamma = T_n/T_e$. The normalized dust grain potential is denoted by $U = e\phi_d/T_e$ and the normalized dust number density by $P = 4\pi r_d \lambda_0^2 n_d$, with $\lambda_0 = (T_e/4\pi n_i Z_i^2 e^2)^{1/2}$. Notice that for $\alpha = 0$ and $q = 1$, $A_{q\alpha} = 1$ and $B_{q\alpha} = 1$, as the result of Eq. (7)

$$I_j^{q\alpha} = n_j q_j \int V_j \sigma_j^{d,f} f_{q\alpha}(V_j) d^3 \mathbf{V}_j. \quad (3)$$

Here, $\sigma_j^d = \pi r_d^2 (1 - 2q_j \phi_d/m_j V_j^2)$ is the cross-section for charging collisions between the dust grains and plasma species of charge q_j , and $\phi_d(r_d)$ is the surface potential (radius) of dust grains. Inserting the value of σ_j^d and $f_{q\alpha}(V_j)$ into Eq. (3) and expressing the spherical volume element ($d^3 \mathbf{V}_j = V_j^3 dV_j d\mu d\phi$), the charging currents due to the electrons and the positive/negative ions for negatively charged dust grains can be expressed, respectively, as

$$I_e^{q\alpha} = -\sqrt{2^3 \pi} r_d^2 \exp\left(\frac{A_{q\alpha} e \phi_d}{B_{q\alpha} m_e V_{Te}^2}\right) n_e V_{Te} B_{q\alpha} Q, \quad (4)$$

$$I_i^{q\alpha} = \sqrt{2^3 \pi} r_d^2 e \left(1 - \frac{A_{q\alpha} Z_i e \phi_d}{B_{q\alpha} m_i V_{Ti}^2} \right) n_i V_{Ti} B_{q\alpha} Q, \quad (5)$$

and

$$I_n^{q\alpha} = -\sqrt{2^3 \pi} r_d^2 e \left(1 + \frac{A_{q\alpha} Z_n e \phi_d}{B_{q\alpha} m_n V_{Tn}^2} \right) n_n V_{Tn} B_{q\alpha} Q, \quad (6)$$

where

$$\begin{aligned} B_{q\alpha} &= \frac{24\alpha + 6 - 17q + 12q^2}{q(-6 + 29q - 46q^2 + 24q^3)}, \\ A_{q\alpha} &= \frac{1 + \frac{8\alpha}{2 + q(-7 + 6q)}}{q} \end{aligned}$$

exactly reducing to Eq. (6) of Ref. 18, i.e., the dust grain surface potential in a Maxwellian dusty plasma. Furthermore, in the absence of negative ion-to-positive ion number density (i.e., $\rho = 0$) and assuming the positive ion to electron ratio approaches the unity (i.e., $\sigma = 1$), Eq. (7) reproduces the result of Ref. 17 for an isolated dust grain. Eq. (7) can be solved numerically to study the variation in the grain surface potential when plasma system is far from thermal equilibrium.

If the negative ion streaming speed V_0 is much larger than negative ion thermal speed, then the negative ion current represented in Eq. (6) can be expressed in the following form

$$I_n^{q\alpha} = -\sqrt{2^3 \pi} r_d^2 Z_n e \left(1 - \frac{A_{q\alpha} Z_n e \phi_d}{B_{q\alpha} m_n V_0^2} \right) n_n V_0 B_{q\alpha} Q. \quad (8)$$

In order to calculate the dust grain surface potential in the presence of streaming of negative ions, we substitute Eqs. (4), (5), and (8) into Eq. (2) to obtain

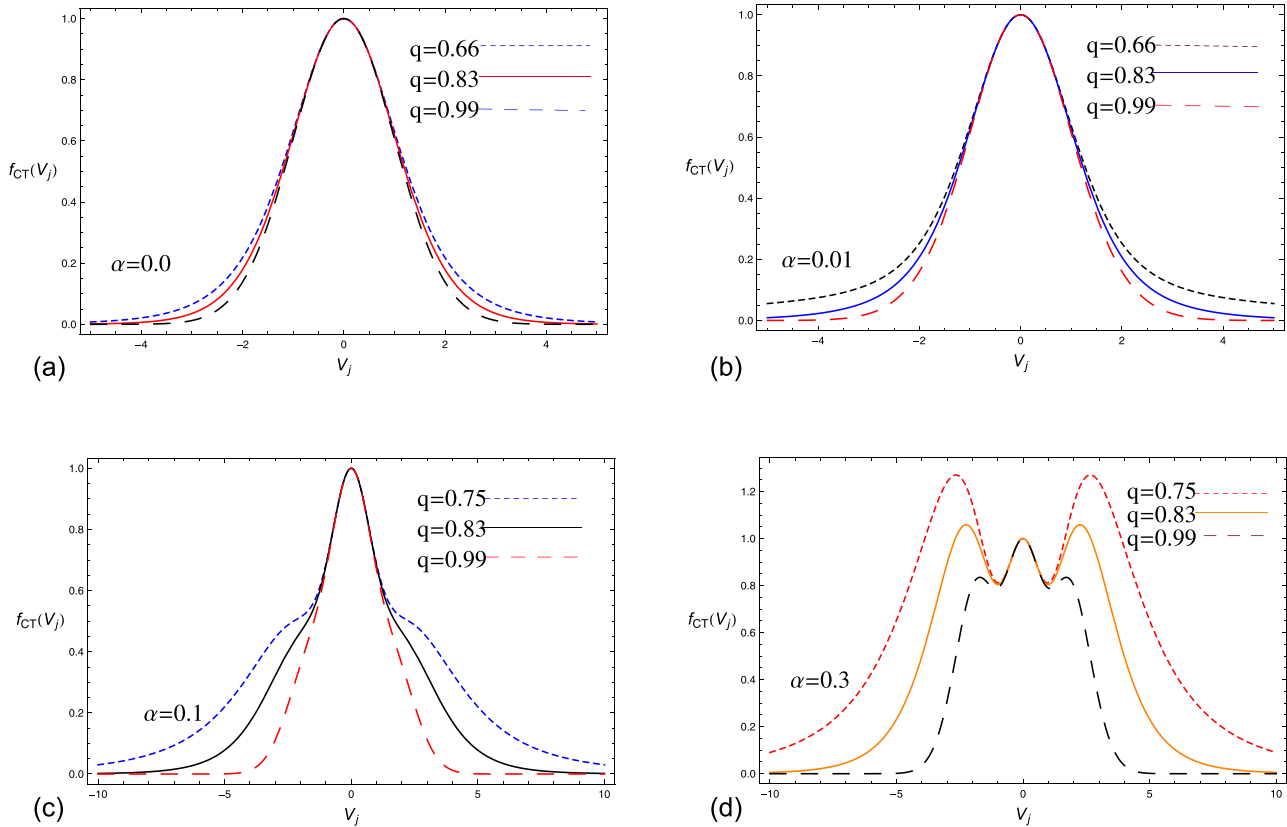


FIG. 1. (a) Normalized Cairns-Tsallis distribution function for the varying spectral index $q(=0.66, 0.83, 0.99)$ with $\alpha=0.0$. (b) Normalized Cairns-Tsallis distribution function for the varying spectral index $q(=0.66, 0.83, 0.99)$ with $\alpha=0.01$. (c) Normalized Cairns-Tsallis distribution function for the varying spectral index $q(=0.75, 0.83, 0.99)$ with $\alpha=0.1$. (d) Normalized Cairns-Tsallis distribution function for the varying spectral index $q(=0.75, 0.83, 0.99)$ with $\alpha=0.3$.

$$\begin{aligned} \sqrt{\sigma} - \frac{A_{qx} Z_i U}{B_{qx} \sqrt{\sigma}} - \mu \left(1 - \rho \frac{Z_n}{Z_i} + Z_i P U \right) \exp \left(\frac{A_{qx}}{B_{qx}} U \right) \\ = \rho \beta \sqrt{U_0} \frac{Z_n}{Z_i} \left(1 + \frac{A_{qx} Z_n U}{B_{qx} U_0} \right), \end{aligned} \quad (9)$$

where $U_0 = m_n V_0^2 / 2T_e$. Eq. (9) represents the equilibrium dust grain surface potential U and normalized dust number density P with streaming of negative ions in the presence of Cairns-Tsallis-distributed plasma. It is observed that by taking the $\alpha=0$ and $q=1$, we have $A_{qx}=1$ and $B_{qx}=1$ since Eq. (9) exactly coincides with Eq. (4) of Ref. 18. Moreover, in the absence of negative ion streaming speed (i.e., $U=0$), negative ion number density ($\rho=0$), and assuming $\sigma \sim 1$, Eq. (9) exactly agrees with the result of Ref. 17. Equation (9) can be solved numerically to study the relation between the grain surface potential and the dust-to-ion number density ratio when plasma system is far away from thermal equilibrium.

IV. NUMERICAL RESULTS AND DISCUSSION

For numerical illustration, we have plotted the normalized Cairns-Tsallis distribution function in Eq. (1) for the different values of q and α . The effect of spectral index α is to increase the high energy particles on the shoulder of the velocity distribution curve, whereas the spectral index q describes the influence of super thermal particles on the tails of the velocity distribution curve. Fig. 1(a) shows the effect

of a pure Tsallis distribution for different values of the parameter q for $\alpha=0$. It is observed that in the Cairns-Tsallis velocity distribution curve approaches to Maxwellian at $q=0.99$. The effect of the nonextensivity parameter q with different values of α is depicted in Figs. 1(b)–1(d). It is observed that for large values of nonthermal $\alpha \neq 0$ affect of plasma species is prominent on the shoulder of the velocity distribution curve. When the contribution of nonextensivity approaches to one q (i.e., $q \sim 1$), the velocity distribution curve approaches the pure Cairns distribution.²²

We have also solved Eqs. (7) and (9) numerically to study dust surface potential U as a function of dust parameter P (dust-to-ion number density ratio) and to examine the various affects of plasma parameters in a non-Maxwellian dusty plasma in Cairns-Tsallis distribution. The latter contains negative and positive ions (O_2^- and O_2^+ ions) in addition to electrons and negatively charged isolated dust grains. Here we have also used some normalized values, which are consistent with the low-temperature laboratory plasmas,^{18,44–46} namely, $\alpha=0.0-0.03$, $\beta=1$, $\gamma=0.1-1$, $\sigma=0.2$, $U_0=0.1-1$, $\rho=0.2-0.6$, and $Z_n=1=Z_i$. Figure 2 exhibits the effects of q on the normalized dust grain surface potential $U = e\phi_d/T_e$ as a function of the normalized dust density parameter $P = 4\pi n_d r_d^2 \lambda_0^2$ [see Eq. (7)], which is now changed with the Cairns-Tsallis distribution for fixed values of $\alpha=0.0$, $\mu=242.8$, $\rho=0.4$, $\beta=1$, $\gamma=0.5$, $\sigma=1.0$, and $Z_i=1=Z_n$. Notice that as we increase the value of q ,

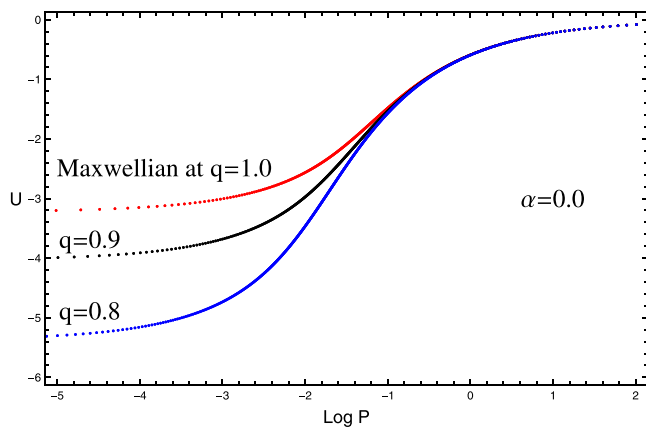


FIG. 2. The equilibrium dust surface potential ($U = e\phi_d/T_e$) against the dust density parameter ($P = 4\pi r_d \lambda_{D0}^2 n_d$) [see Eq. (7)] for the different values of spectral index $q = (0.8, 0.9, 1.0)$. Other parameters used here are $\alpha = 0.0$, $\sigma = 1.0$, $\rho = 0.4$, $\beta = 1$, $\gamma = 0.5$, $\mu = 282.8$, and $Z_i = 1 = Z_n$.

the magnitude of dust grain surface potential decreases and the curves tend to approach the Maxwellian case when $q = 1$, whereas opposite behavior is obtained by increasing the value of the positive ion-to-electron temperature ratio σ and spectral index α , shown in Figs. 3 and 4 in the presence of Boltzmannian negative ions. On the other hand, Fig. 5 illustrates how the value of q affects the dust surface potential or dust charge in the presence of streaming of negative ions with the fixed value of α [see Eq. (9)]. It is investigated that as we increase the value of q , the dust surface potential decreases. Fig. 6, on the other hand, depicts the behavior of negative ion streaming speed (U_0) on the dust grain potential. It is observed that as we increase the value of U_0 with fixed value of $\alpha = 0.01$ and $q = 0.9$, the dust surface potential increases.

In conclusion, we have considered two models for negative ions, the streaming negative ions and the Boltzmannian negative ions, to investigate their effects on the charging of dust grain in non-Maxwellian dusty plasmas with Cairns-Tsallis-distribution function. We derive the expressions for the dust grain surface potential by solving the current balance equations for the Cairns-Tsallis distributed plasma with

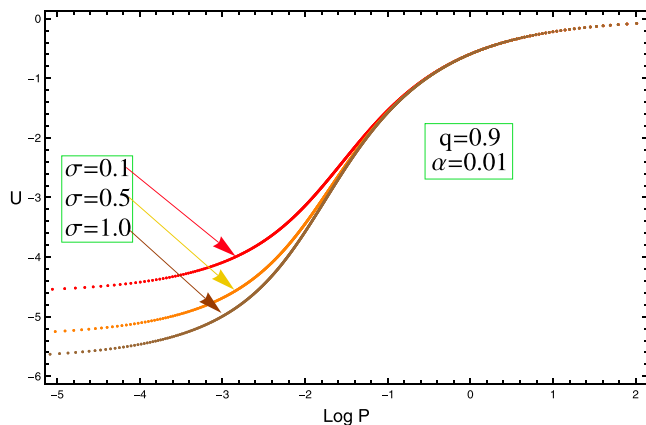


FIG. 3. The equilibrium dust surface potential ($U = e\phi_d/T_e$) against the dust density parameter ($P = 4\pi r_d \lambda_{D0}^2 n_d$) [see Eq. (7)] for the different values of the positive ion-to-electron temperature ratio $\sigma = (0.1, 0.5, 1.0)$ with $q = 0.9$ and $\alpha = 0.01$. Other parameters used here are same as in Fig. 1.

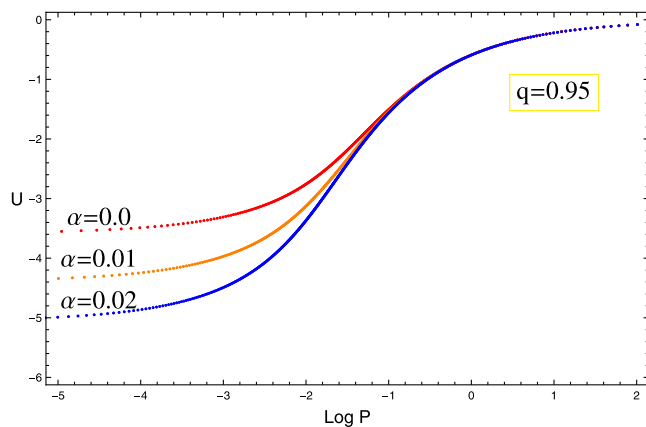


FIG. 4. The equilibrium dust surface potential ($U = e\phi_d/T_e$) against the dust density parameter ($P = 4\pi r_d \lambda_{D0}^2 n_d$) [see Eq. (7)] for different values of $\alpha = (0.0, 0.01, 0.02)$ with $q = 0.95$. Other parameters used here are same as in Fig. 1.

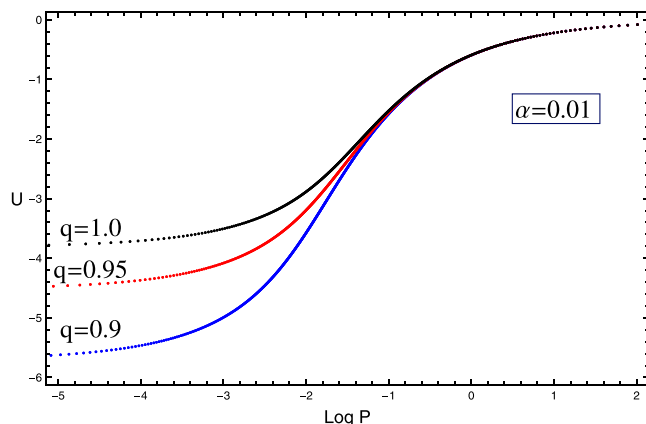


FIG. 5. The equilibrium dust surface potential ($U = e\phi_d/T_e$) against the dust density parameter ($P = 4\pi r_d \lambda_{D0}^2 n_d$) [see Eq. (9)] for different values of spectral index $q = (0.9, 0.95, 1.0)$ with $\alpha = 0.01$ and $U_0 = 1$. Other parameters used here are as in Fig. 1.

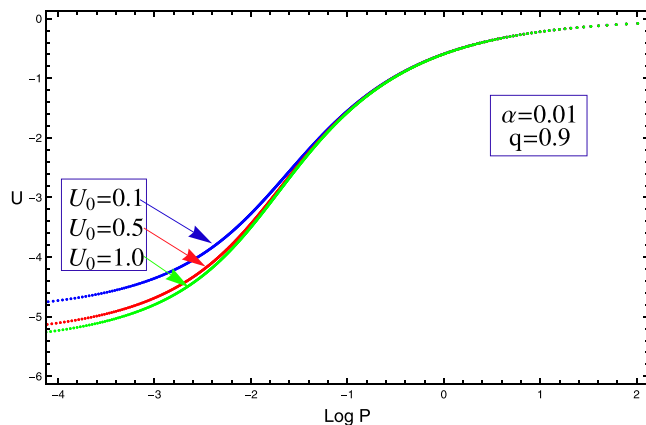


FIG. 6. The equilibrium dust surface potential $U = e\phi_d/T_e$ against the dust density parameter ($P = 4\pi r_d \lambda_{D0}^2 n_d$) [see Eq. (9)] for different values of the negative ion streaming speed $U_0 = (0.1, 0.5, 1.0)$ with $q = 0.9$ and $\alpha = 0.01$. Other parameters used here are same as in Fig. 1.

spectral indexes (α , q) due to the electrons and positive/negative ions. Numerical calculations reveal that the variation of plasma parameters, such as the spectral indexes (α , q), the positive ion-to-electron temperature ratio σ , and the negative ion streaming speed U_0 significantly affect the dust surface potential. By increasing the values of spectral index α , positive ion-to-electron temperature ratio σ , and the negative ion streaming speed U_0 , the magnitude of the equilibrium dust surface potential increases, while the increase of the spectral index q shows the opposite effects.

ACKNOWLEDGMENTS

This project was supported by Grant Nos. UM.C/625/1/HIR/MOE/SC/33/1 and RP008C-13AFR and by Project Nos. UID/Multi/00491/2013 and UID/EEA/50008/2013.

- ¹P. K. Shukla and A. A. Mamun, *Introduction to Dusty Plasma Physics* (IOP Publishing Ltd., Bristol, 2002).
- ²M. Horanyi and D. A. Mendis, *Astrophys. J.* **294**, 357 (1985).
- ³C. K. Goertz, *Rev. Geophys.* **27**, 271, doi:10.1029/RG027i002p00271 (1989).
- ⁴V. E. Fortov, A. V. Ivlev, S. A. Khrapak, A. G. Khrapak, and G. E. Morfill, *Phys. Rep.* **421**, 1 (2005).
- ⁵N. N. Rao, P. K. Shukla, and M. Y. Yu, *Planet. Space Sci.* **38**, 543 (1990).
- ⁶P. K. Shukla and L. Steno, *Astrophys. Space Sci.* **190**, 23 (1992).
- ⁷A. Barkan, R. L. Merlino, and N. D'Angelo, *Phys. Plasmas* **2**, 3563 (1995).
- ⁸A. A. Mamun, M. Salahuddin, and M. Salimullah, *Planet. Space Sci.* **47**, 79 (1998).
- ⁹F. Melands, T. K. Aslaksen, and O. Havnes, *Planet. Space Sci.* **41**, 321 (1993).
- ¹⁰M. Rosenberg, *Planet. Space Sci.* **41**, 229 (1993).
- ¹¹N. D'Angelo, *J. Phys. D* **28**, 1009 (1995).
- ¹²B. Feuerbacher, R. T. Willis, and B. Fitton, *J. Astrophys.* **181**, 101 (1973).
- ¹³H. Fechtig, E. Grun, and G. E. Morfill, *Planet. Space Sci.* **27**, 511 (1979).
- ¹⁴O. Havnes, C. K. Goertz, G. E. Morfill, E. Grun, and W. Ip, *J. Geophys. Res.* **92**, 2281, doi:10.1029/JA092iA03p02281 (1987).
- ¹⁵M. S. Barnes, J. H. Keller, J. C. Forster, J. A. O'Neil, and D. K. Coultas, *Phys. Rev. Lett.* **68**, 313 (1992).
- ¹⁶B. Walch, M. Horanyi, and S. Robertson, *Phys. Rev. Lett.* **75**, 838 (1995).
- ¹⁷A. Barkan, N. D'Angelo, and R. L. Merlino, *Phys. Rev. Lett.* **73**, 3093 (1994).
- ¹⁸A. A. Mamun and P. K. Shukla, *Phys. Plasmas* **10**, 1518 (2003).
- ¹⁹A. A. Abid, S. Ali, and R. Muhammad, *J. Plasma Phys.* **79**, 1117 (2013).
- ²⁰R. Bostrom, *IEEE Trans. Plasma Sci.* **20**, 756 (1992).
- ²¹P. O. Dovner, A. I. Eriksson, R. Bostrom, and B. Holback, *Geophys. Res. Lett.* **21**, 1827, doi:10.1029/94GL00886 (1994).
- ²²R. A. Cairns, A. A. Mamun, R. Bingham, R. Bostrom, R. O. Dendy, C. M. C. Nairn, and P. K. Shukla, *Geophys. Res. Lett.* **22**, 2709, doi:10.1029/95GL02781 (1995).
- ²³A. A. Mamun, *Eur. Phys. J. D* **11**, 143 (2000).
- ²⁴X. Jukui, *Chaos, Solitons Fractals* **18**, 849 (2003).
- ²⁵S. Maharaj, S. Pillay, R. Bharuthram, R. Reddy, S. Singh, and G. Lakhina, *J. Plasma Phys.* **72**, 43 (2006).
- ²⁶T. K. Baluku and M. A. Hellberg, *Plasma Phys. Controlled Fusion* **53**, 095007 (2011).
- ²⁷F. Verheest and S. Pillay, *Phys. Plasmas* **15**, 013703 (2008).
- ²⁸F. Verheest and M. A. Hellberg, *Phys. Plasmas* **17**, 102312 (2010).
- ²⁹A. A. Mamun and P. K. Shukla, *Phys. Rev. E* **80**, 037401 (2009).
- ³⁰S. Yasmin, M. Asaduzzaman, and A. A. Mamun, *Phys. Plasmas* **19**, 103703 (2012).
- ³¹M. Asaduzzaman and A. A. Mamun, *Phys. Rev. E* **86**, 016409 (2012).
- ³²C. Tsallis, *J. Stat. Phys.* **52**, 479 (1988).
- ³³J. A. S. Lima, R. Silva, Jr., and J. Santos, *Phys. Rev. E* **61**, 3260 (2000).
- ³⁴L. Liu and J. Du, *Physica A* **387**, 4821 (2008).
- ³⁵P. Eslami, M. Mottaghizadeh, and H. Pakzad, *Phys. Plasmas* **18**, 102303 (2011).
- ³⁶M. Tribeche, L. Djebarni, and H. Schamel, *Phys. Lett. A* **376**, 3164 (2012).
- ³⁷M. Tribeche, L. Djebarni, and R. Amour, *Phys. Plasmas* **17**, 042114 (2010).
- ³⁸V. Vasyliunas, *J. Geophys. Res.* **73**, 2839, doi:10.1029/JA073i009p02839 (1968).
- ³⁹G. Livadiotis and D. J. McComas, *J. Astrophys.* **741**, 88 (2011).
- ⁴⁰A. A. Abid, S. Ali, J. Du, and A. A. Mamun, *Phys. Plasmas* **22**, 084507 (2015).
- ⁴¹G. Williams, I. Kourakis, F. Verheest, and M. A. Hellberg, *Phys. Rev. E* **88**, 023103 (2013).
- ⁴²M. Tribeche, R. Amour, and P. K. Shukla, *Phys. Rev. E* **85**, 037401 (2012).
- ⁴³N. Rubab and G. Murtaza, *Phys. Scr.* **73**, 178 (2006).
- ⁴⁴H. Amemiya, B. M. Annaratone, and J. E. Allen, *J. Plasma Phys.* **60**, 81 (1998).
- ⁴⁵H. Amemiya, B. M. Annaratone, and J. E. Allen, *Plasma Sources. Sci. Technol.* **8**, 179 (1999).
- ⁴⁶V. Vyas, G. A. Hebner, and M. J. Kushner, *J. Appl. Phys.* **92**, 6451 (2002).